A modular cell culture device for generating arrays of gradients using stacked microfluidic flows

Christopher G. Sip, Nirveek Bhattacharjee, and Albert Folch[a)]
Department of Bioengineering, University of Washington, Seattle, Washington 98195, USA

(Received 16 December 2010; accepted 6 March 2011; published online 29 June 2011)

Microfluidics has become increasingly important for the study of biochemical cues because it enables exquisite spatiotemporal control of the microenvironment. Well-characterized, stable, and reproducible generation of biochemical gradients is critical for understanding the complex behaviors involved in many biological phenomena. Although many microfluidic devices have been developed which achieve these criteria, the ongoing challenge for these platforms is to provide a suitably benign and physiologically relevant environment for cell culture in a user-friendly format. To achieve this paradigm, microfluidic designs must consider the full scope of cell culture from substrate preparation, cell seeding, and long-term maintenance to properly observe gradient sensing behavior. In addition, designs must address the challenges associated with altered culture conditions and shear forces in flow-based devices. With this consideration, we have designed and characterized a microfluidic device based on the principle of stacked flows to achieve highly stable gradients of diffusible molecules over large areas with extremely low shear forces. The device utilizes a benign vacuum sealing strategy for reversible application to pre-established cell cultures. We apply this device to an existing culture of breast cancer cells to demonstrate the negligible effect of its shear flow on migratory behavior. Lastly, we extend the stacked-flow design to demonstrate its scalable architecture with a prototype device for generating an array of combinatorial gradients. [doi:10.1063/1.3576931]

I. INTRODUCTION

Observation of how cells polarize or migrate in response to biomolecular gradients is critical for the study of complex phenomena such as development, neuronal path finding, immune response, regeneration, and cancer. Much of the fundamental understanding of these systems has been accomplished *in vitro* using dissociated cell cultures or explants and careful manipulation of the cellular microenvironment. Some of the well-known methods for observing gradient sensing are hydrogels,[1] micropipettes,[2] permeable membrane assays,[3] and chemotaxis chambers.[4] These traditional platforms for gradient generation have enabled researchers to identify biomolecules and mechanisms involved in gradient detection and signaling. However, more sophisticated manipulation of chemical concentrations and quantifiable methods are desired to further elucidate these phenomena. Recently, microfluidic technology with its intrinsic capability for spatial and temporal control has gained popularity for gradient studies.[5] The generation of stable, quantifiable, and reproducible gradients has been demonstrated by a variety of microfluidic devices.

One of the most popular gradient generator designs is the "premixer" style device developed by Dertinger *et al.*[6] Using the splitting and recombining of microchannel flow, these types of devices are capable of generating gradients of arbitrary shapes from a few concentration inputs.[7] These devices have been used for a variety of studies, including neutrophil chemotaxis,[8] differentiation,[9] and cancer cell migration;[10] however, limitations of enclosed microchannel cell

[a)]Electronic mail: afolch@u.washington.edu.

culture and shear flow confounding cell responses have led to the development of a second generation of microfluidic devices.[11] Several of these designs incorporate high-resistance microchannels[12–14] or porous barriers such as gels or membranes[15–18] to limit the exposure of cell cultures to shear forces. In order to avoid problems with enclosed channel designs, some designs utilize open microchambers to facilitate cell seeding and culture.[12,14,18–20] Another effective solution has been to implement reversible sealing techniques such as clamping[21,22] or vacuum sealing,[23–26] which simplify integration of cell cultures with "add-on" microfluidic devices. More importantly, none of the devices presented to date has an architecture that is amenable to combinatorial testing of various gradients. Microfluidic gradient generators continue to be used for identifying critical gradients and their complex effects; however, the ongoing challenge is to maintain a suitably benign and physiological relevant environment for cell culture in a high-throughput, combinatorial, and user-friendly format.

In this paper, we present a microfluidic gradient platform that features extremely low shear forces and simple interfacing with cultures. In our device, gradient generation is based on the principle of stacked laminar flows to produce stable gradients of diffusible molecules over a 4 mm^2 area for 24 h with negligible shear forces ($\sim 6 \times 10^{-3}$ dyn/cm^2). In addition, we integrate a vacuum sealing feature for reversible application of the device to pre-established cell cultures, so cells do not need to be introduced into the device through a dedicated inlet. We demonstrate the long-term stability and dynamic tunability of gradients produced using the stacked-flow device. We also show that the application of this device to pre-existing cultures of breast cancer cells is straightforward. Furthermore, our microfluidic architecture is designed for generating arrays of combinatorial gradients, which we demonstrate as a proof of concept.

II. EXPERIMENTAL

A. Materials

SU-8 2000 series photoresists were obtained from MicroChem (Newton, MA). Dow Corning Sylgard 184 poly(dimethyl siloxane) (PDMS) was purchased from KR Anderson, Inc. (Kent, WA). Fluorosilane [(Tridecafluoro-1,1,2,2, tetrahydrooctyl)-1 trichlorosilane] was obtained from United Chemical Technologies, Inc. (Horsham, PA). Orange-G dye, fluorescein sodium salt, bovine serum albumin (BSA), poly-D-lysine, and collagen type IV were purchased from Sigma-Aldrich (St. Louis, MO). GIBCO™ brand RPMI 1640 medium was obtained from Invitrogen (Carlsbad, CA). MDA-MB-231 breast cancer cells were supplied by American Type Cell Culture Collection (Manassas, VA). Polyester liner sheets, Scotchpack™ 9744 Release Liner, were generously donated by 3M (St. Paul, MN). 3-aminopropyltriemethoxysilane (APTES) and 3-glycidyloxypropyltrimethoxysilane (GPTMS) were purchased from Sigma-Aldrich.

B. Fabrication

Fabrication of the vacuum sealing stacked-flow device follows the principles of soft-lithography and the layer-by-layer assembly scheme outlined in Figs. 1(a)–1(h). Fabrication of the device begins with the preparation of a set of three multilayer SU-8 patterned master molds using two-step photolithography. Each device is assembled from replicas of these molds produced in PDMS. The top flow layer is defined by casting a thick replica with PDMS several millimeter thick. The bottom flow and vacuum sealing layers were each produced by "exclusion molding" PDMS between the masters and a polyester liner sheet by applying force with a clamp.[19] The tallest SU-8 features exclude PDMS completely from the liner sheets, thereby resulting in perforated and patterned membranes. Inlets, outlets, and vacuum ports are cored into the top flow layer using a biopsy punch (Harris Uni-core, Ted-Pella, Redding, CA). Each layer is aligned and bonded in two subsequent plasma oxidation steps to complete the device.

To produce arrays of stacked-flow gradient generators, we used a similar fabrication scheme with a few exceptions. Instead of vacuum sealing, this particular device was produced with enclosed channels for the purpose of demonstrating the three-dimensional (3D) microfluidic plumbing and the generation of multiple combinatorial gradients. For this device, the layers were

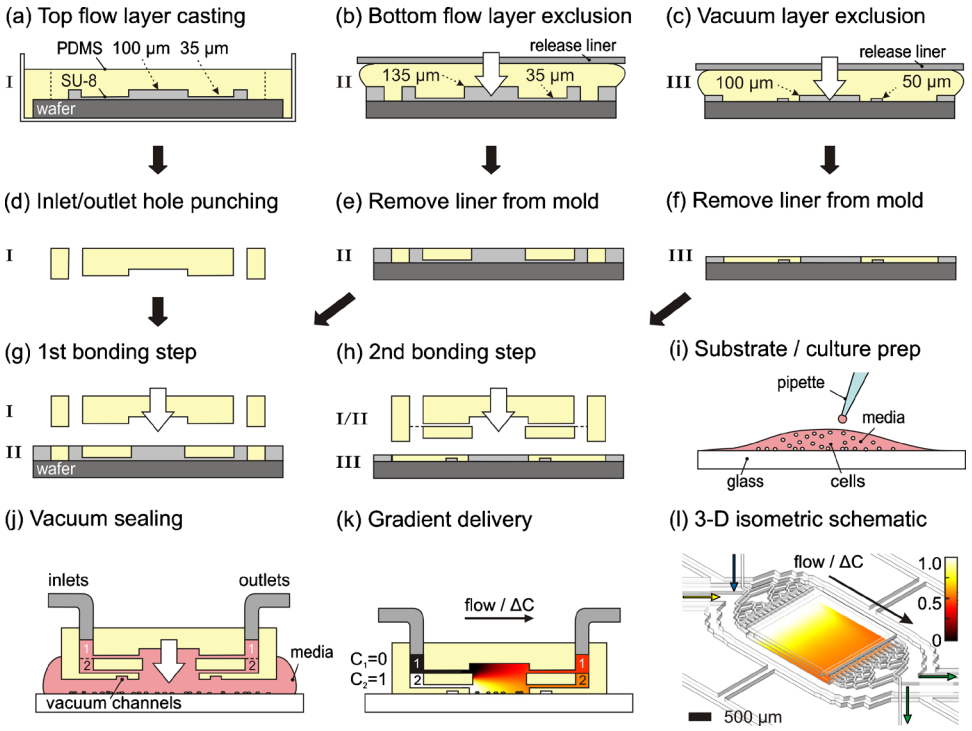

FIG. 1. Schematic illustration of fabrication process and operation of the vacuum sealing stacked-flow gradient device. (a) For the top flow layer, a thick replica mold is cast by curing PDMS over a multilayer SU-8 patterned mold. [(b) and (c)] The bottom flow and vacuum layers are exclusion-molded by clamping PDMS between a patterned wafer and a polyester liner. The tallest SU-8 features exclude PDMS completely from the layer, resulting in a perforated and patterned membrane. (d) Inlets are bored in the top flow layer for fluidic access. [(e) and (f)] The liners are removed from the molds to expose the top side of the PDMS membranes. [(g) and (h)] Layer-by-layer bonding is achieved with two plasma oxidation steps. (i) Substrates are prepared on glass for cell seeding and culture prior to application of the device. (j) Integrated vacuum sealing channels enable the wet application of the device to an established cell culture. (k) Stacked flow is delivered to generate a gradient at the cell culture surface. (l) A 3D isometric schematic shows the structure of the device with a simulated gradient for fluorescein (MW: 332.31 and diffusivity $D \sim 6.4 \times 10^{-6}$ cm^2/s) superimposed at the cell culture surface.

bonded using a room temperature chemical bonding technique involving amino-epoxy reactive chemistry.[27,28] To functionalize the PDMS surfaces with either amino- and epoxy-reactive groups, plasma oxidized layers were immersed for 20 min in solutions of either 1% APTES in water or 1% GPTMS in ethanol, respectively. Complementary pairs of treated PDMS layers were then rinsed with distilled water, air dried, and brought into conformal contact to achieve bonding after several hours at room temperature. This method enables careful alignment and construction of large multilayer devices because the bonding is not instantaneous like with pure oxidative plasma bonding technique.

C. Device operation

The vacuum sealing feature of the device enables the straightforward preparation of substrates and cell seeding, as shown in Fig. 1(i). The device contains a rectangular open chamber 300 μm deep and 4 mm^2 in area, which interfaces directly with cell culture substrates through vacuum sealing, as shown in Fig. 1(j). By reversible application of the device, we can introduce soluble gradients at any time point to pre-established cell cultures given a flat substrate suitable for sealing. During operation of the device, as shown in Fig. 1(k), two stacked flows are generated in the square cell culture chamber with each flow serving as a source or a sink for a soluble factor. A concentration gradient is formed simply by diffusion between the laminar streams as they flow through the chamber and toward the outlets. This produces a steady-state and large-area concen-

tration gradient at the cell substrate surface. In essence, the gradient generator's primary feature is the reliance on the slow diffusive broadening (in the direction orthogonal to the surface) of the concentration boundary formed by the two adjacent streams. Incidentally, diffusive broadening is a significant limiting factor for the popular "Dertinger style" of gradient generator devices.[6]

D. Finite-element modeling

We used finite-element modeling (FEM) software (COMSOL MULTIPHYSICS 3.3, COMSOL, Inc., Burlington, MA) in order to predict the microfluidic behavior of the stacked-flow device. The device was modeled in two-dimensions (2D) as an infinite slit using the previously described methods.[12] The driving pressure of the model has to be reduced by a factor to compensate for the lower fluidic resistance of the infinite slit. Using experimental data gathered for gradient shape, the scaling factor can be estimated in order provide an appropriate driving pressure for the model. The model provides knowledge of the fluid flow and the shear forces at the surface in the cell culture chamber.

E. Surface gradient detection

In order to quantify the gradients generated by the device, we utilized an epifluorescence surface imaging technique to collect intensity data from an approximately $\sim 4.9\ \mu$m optical slice.[29] Concentrated solutions of 45 mM Orange-G were introduced into the device in both flow channels with one channel containing 1 mM fluorescein. The fluorescein source channel was configured at either the top or bottom flow levels to generate directionally different gradients. Data were collected at various driving pressures, while equilibration times and stability were evaluated with time-lapse imaging.

F. Cell culture and time-lapse imaging

Cell culture medium was prepared from fresh RPMI 1640 supplemented with 2.05 mM L-glutamate, 1% penicillin-streptomycin, and 25 mM 4-(2-hydroxyethyl)-1-piperazineethanesulfonic acid (HEPES) buffer. Cell culture substrates were prepared from clean glass slides coated with poly-D-lysine at 10 μg/ml for 1 h at 37 °C, rinsed thoroughly with phosphate buffered saline (PBS), and then coated with collagen type IV at 2 μg/ml overnight at 37 °C. MDA-MB-231 breast cancer cells were dissociated in cell dissociation buffer and then plated at $\sim$70 000 cells/slide in 300 μl on the substrates. Seeded substrates were cultured for 24 h in a 37 °C and 5% CO_2 controlled incubator before application of the vacuum sealing device. In preparation for applying to cell cultures, the device was vacuum-sealed to a blank substrate and primed by flowing 2% BSA solution through the channels for several hours, then replaced with medium containing 0.1% BSA, and debubbled. The device is then released from its loading substrate and allowed to form a droplet of medium at the open surface of the cell culture chamber. Next, the device is carefully lowered onto the cell culture substrate, while the droplet ensures that no air bubbles remain trapped within the chamber or contact with the cells. It is critical to allow flow through the device at a low driving pressure (0.2 psi) to prevent depressurization of the cell culture compartment when the vacuum channels seal against the substrate. The vacuum sealing operation is conducted under wet conditions, thereby maintaining the supportive environment for the cells. Phase-contrast images were collected every 5 min over the course of 12 h to track migration of the cells. METAMORPH (Molecular Devices, Inc., Sunnyvale, CA) was used to threshold, segment, and register the centroid of the cells in all the frames and MATLAB (MathWorks, Natick, MA) was used to analyze the data and track the trajectories of the centroids. The tracking algorithm started with the centroids registered in the last frame and worked recursively backward to identify the nearest centroid in the previous frame, which belonged to a cell with similar attributes (area and perimeter). This ensured that we analyzed only the cells, which remained in the frame for the entire 12 h window.

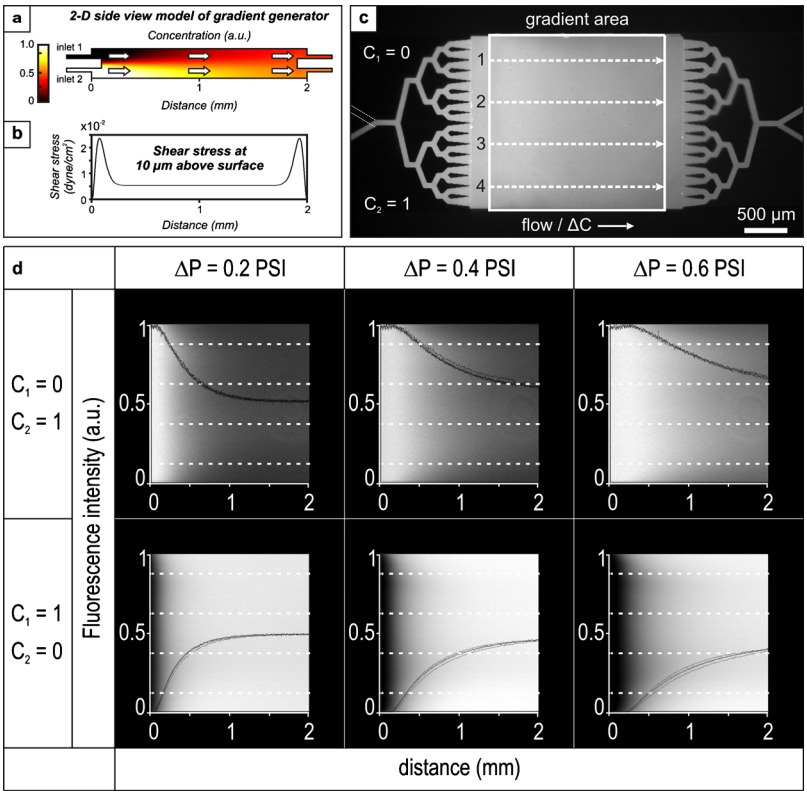

FIG. 2. Finite-element modeling and fluorescence characterization of surface gradients. (a) A 2D model of the stacked-flow device is shown here with a representative gradient generated with fluorescein as the diffusing species (MW: 332.31 and $D \sim 6.4 \times 10^{-6}$ cm^2/s) delivered via the bottom inlet. (b) The shear stress predicted for 10 μm above the surface is $\sim 6 \times 10^{-3}$ dyn/cm^2, two orders of magnitude below the threshold for inducing neutrophil migration bias (~ 0.7 dyn/cm^2) (Ref. 30). (c) A typical surface-level fluorescence micrograph of the device highlights the gradient area (box) and the locations of the intensity profile analysis (dotted lines). (d) In each of the six panels, a fluorescence micrograph of the surface gradient area is superimposed with four corresponding intensity profiles (taken across the dashed horizontal white lines) in order to demonstrate lateral uniformity. The gradient can be dynamically tuned by the driving pressure, ΔP, and the direction of the gradient is dependent on the inlet configuration.

III. RESULTS AND DISCUSSION

A. FEM predicts wide-area gradients and low shear forces at the surface

The fluid dynamics for the stacked flows can be understood by the 2D simulation shown in Figs. 2(a) and 2(b). As shown here, the model is solved with fluorescein as the diffusing species (MW: 332.31 and diffusivity $D \sim 6.4 \times 10^{-6}$ cm^2/s) delivered via the bottom inlet. In practice, the device is operated near driving pressures at which the stacked flows evolve into a homogeneous or fully mixed solution when they pass through the outlet of the gradient chamber; therefore, the driving pressures for the model were chosen to mimic this condition. Using this guideline, simulations were produced to predict the fluid shear stresses for gradients generated with different diffusing species at a distance of 10 μm above the cell culture surface. With fluorescein, the model predicts shear stresses of $\sim 6 \times 10^{-3}$ dyn/cm^2 for 70% of the chamber length. At already two orders of magnitude below the reported threshold for inducing migration bias (~ 0.7 dyn/cm^2), the device is expected to be suitable for sensitive chemotaxis experiments.[30] In practice, for most proteins that diffuse slowly (e.g., the diffusivity of albumin is $D \sim 6.4 \times 10^{-7}$ cm^2/s), the gradient is generated at very small flow rates, so the shear stresses involved are another order of magnitude smaller.

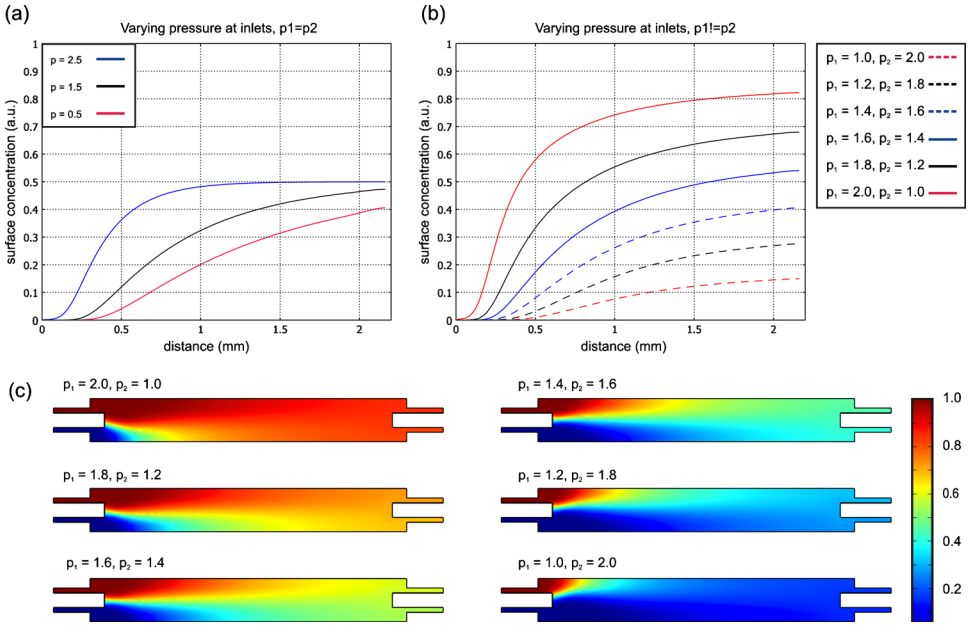

FIG. 3. Finite-element modeling of surface gradients generated using stacked flows demonstrates dynamic tunability. Each of the series of plots was generated using fluorescein as the diffusing species (MW: 332.31 and $D \sim 6.4 \times 10^{-6}$ cm^2/s). Driving pressures are unadjusted values from the 2D simulation. In all simulations shown here, the inlets were configured as $C_1 = 1$ and $C_2 = 0$. (a) A plot of surface concentration profiles generated for different driving pressures applied equally to each inlet. See Fig. 2(d) for a comparison to the experimentally acquired results. (b) A plot of surface concentration profiles generated with driving pressures applied differentially to each inlet. Notice that differential driving pressures enables further flexibility in the maximum concentration range imposed across the surface. (c) Cross-sectional plots are shown with a thermal map of the concentration profile throughout the microchannel for various pressure configurations.

B. Large-area surface gradients can be dynamically tuned

Surface-level gradients were quantified using an imaging technique for adapting regular epi-fluorescence microscopy to collect surface-level intensity.[29] We can limit the penetration length of the excitation light into our sample by flowing a mixture of nonfluorescent and fluorescent dyes, Orange-G and fluorescein, respectively. The dyes are chosen because Orange-G absorbs strongly at the excitation wavelength (490 nm) and weakly at the emission wavelength of fluorescein (540 nm). In combination, the fluorescein dye competes with the Orange-G in solution for a finite amount of excitation energy. At a concentration of 45 mM for Orange-G with a 0.6 numerical aperure objective, the characteristic penetration length is approximately 4.9 μm (for which the excitation light intensity is 1/e times the incident intensity of the excitation light).[14] Since the intensity of the excitation light decays exponentially the farther it penetrates the solution, 95% of the collected emission light $(1-1/e^3)$ is from within $\sim$15 μm of the surface of the device, as shown in the example of Fig. 2(c). Using this technique, we characterized the stacked-flow gradients at different driving pressures and orientations of the source and sinks using fluorescein and Orange-G, as shown in Fig. 2(d). We found the surface gradients produced to be stable over 24 h and reach equilibrium quickly (less than 5 min). Across the width, the gradients were highly uniform as demonstrated by the overlapping profiles of the intensity plots in each panel of Fig. 2(d). Furthermore, the gradients are dynamically tunable with the shape responding to the applied driving pressure as a result of the competing nature of the convection and interdiffusion of the laminar flows. Additional flexibility in the gradient profiles can be achieved by independently controlling the driving pressures applied at the inlets, as shown in Fig. 3. This feature is important because a range of gradient slopes can be tested during the course of a time lapse to help determine the critical conditions for a particular cell-based assay.

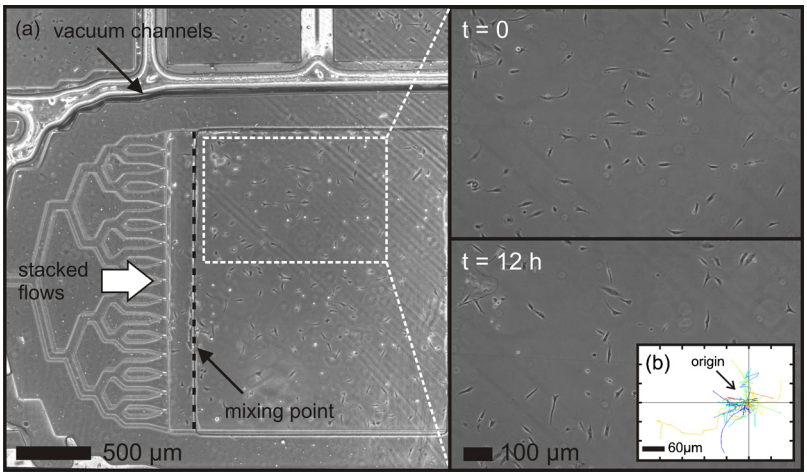

FIG. 4. Vacuum sealing of the stacked-flow device to an established culture of MDA-MB-231 breast cancer cells. A phase-contrast micrograph of the device is shown on the left at low magnification to display the geometry of the device in relation to the cell culture. During application of the device, the vacuum channels apply suction to the substrate in order to actively seal the open surface of the device against the substrate. After sealing, the cell culture is compartmentalized into the microfluidic channel. Our method of reversible sealing is notably benign with evidence of healthy breast cancer cells in the device for 12 h as shown in the inset. The lower right inset shows the trajectories of 26 cells, over 12 h, with their initial positions collapsed onto the origin. It clearly shows that the flow through the chamber does not introduce any migrational bias in the cells. Phase-contrast images were collected every 5 min over the course of 12 h to track migration of the cells. The resulting movie is shown at 7 frames/s with 140 total frames (enhanced online).
[URL: http://dx.doi.org/10.1063/1.3576931.1]

C. Vacuum sealing operation and stacked flow is benign to cell culture preparations

A prevailing drawback of other gradient generator devices is the required adaptation of cell culture protocols for "closed" microchannel designs. Optimizing culture conditions is increasingly difficult for sensitive cell types such as primary cultures, which has led to the popularity of open-access designs.[5,11] However, a salient feature of our device is the reversible sealing design that foregoes the adaptation of cell culture protocols. Importantly, the design enables the temporary application of the device and continued culture after gradient application. After removing the device to continue cell culture, we found that rinsing the substrate with fresh culture medium was adequate to remove the cells damaged beneath the sealing surface of the device. We think that these cells are either crushed or sheared away by the vacuum sealing action and, therefore, can be easily detached from the surface. Replenishing the cell culture with fresh medium removes any harmful factors that can potentially be released from the damaged or dead cells. Likewise, during application of the device, the continuous flow of fresh medium negates the possible effects of the damaged cells around the edge of the chamber boundary. The vacuum sealing operation was tested for pre-established cultures of MDA-MB-231 breast cancer cells. We chose this cell type in order to quantify the effects of shear flow on the random migration behavior. Cells were plated at low density on collagen-coated glass slides 24 h prior to application of the device. We show in Fig. 4 that the application of the device does not interfere with the random migratory (chemokinesis) behavior of the cells over long-term application (see a time-lapse movie). Additionally, the application of stacked flow did not introduce migratory bias for these cells because it exerts negligible shear forces. Importantly, what we demonstrate is that our "closed" stacked-flow microchannel design is benign to cell culture preparations through the careful consideration of fluid flows and interfacing methods.

D. Scalable architecture enables arrays of multiple gradients

To demonstrate the scalable architecture of our design, we fabricated devices with 2×2 and 4×4 arrays of stacked-flow gradient generators. In the 2×2 array design shown in Fig. 5(a), blue

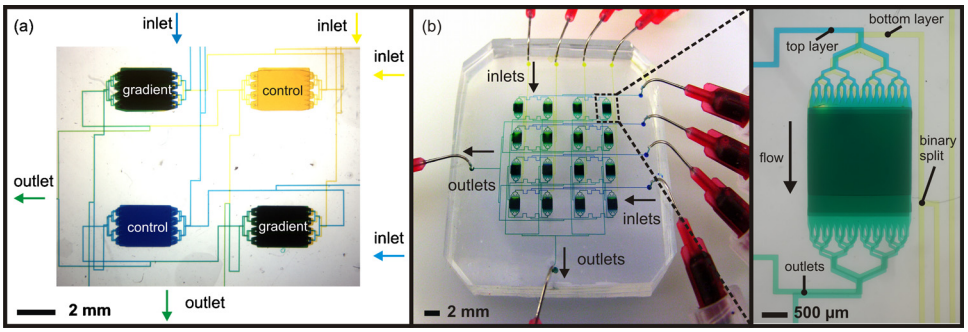

FIG. 5. The scalable stacked-flow architecture enables arrays of gradient generators for high-throughput screening. (a) A 2×2 array of gradient generators is shown with yellow and blue dye representing different concentrations of a gradient molecule. Across the diagonal of the array, these elements serve as controls for different baseline concentrations (yellow and blue), whereas the remaining elements are complementary pairs of gradients (green). (b) A wide-field image of a 4×4 array device highlights the inherent scalability of the microchannel architecture. To visualize the overlapping flow, blue and yellow dyes are introduced into the row and column inlets (top and bottom layers), respectively. At each gradient chamber, the top and bottom flows combine to produce a green solution at the outlets. In the inset on the right, a single gradient generator is shown to highlight the architecture of the individual elements.

and yellow dyes were introduced to visualize the flow. One can imagine assays where the dyes represent different chemical titrations of the same molecule, producing different gradient combinations at each element of the array. Across the diagonal of the array, equal concentrations would flow into the chambers to serve as controls for baseline concentrations; meanwhile, different concentrations intersect to produce complementary pairs of stacked-flow gradients. To further demonstrate scalability, we extended this design to produce a 4×4 array device, as shown in Fig. 5(b). To highlight the 3D microplumbing, blue and yellow dyes were introduced at the row and column inlets, respectively. Careful design of the microchannel network with binary branching was used to ensure that each fluidic path from any inlet to the outlets is equivalent. These proof-of-concept devices show that our platform can be adapted for assaying of a wide range of gradients simultaneously. This feature would have particular utility when biologically relevant concentrations of a chemical cue are unknown; with high-throughput screening of gradients, we could pinpoint the critical concentrations which elicit a response from cells.

IV. CONCLUSIONS

We have demonstrated a low shear gradient generator design with vacuum sealing for straightforward interfacing with cell cultures. The modular nature of our device can allow for more advanced preparation of substrates and cell cultures such as patterning or differentiation because it does not interfere with standard protocols. The device sealing is reversible, which allows for further treatment of the cell cultures after exposure to the gradient. We have shown that the gradients are highly stable over 24 h and uniform, which is ideal for quantitative analysis. With the scalability of the stacked-flow design, we could generate arrays of gradients for high-throughput screening. Further development of the array devices to incorporate vacuum sealing could allow for such experiments. We believe that the design principles demonstrated here are important for the microfluidic community interested in the development of user-friendly devices and for disseminating our technology to non-microfabrication oriented laboratories.

ACKNOWLEDGMENTS

Support for this work was generously provided by the National Institutes of Health/National Institute of Biomedical Imaging and Bioengineering (Grant No. R21/R33 EB003307).

[1] R. D. Nelson, P. G. Quie, and R. L. Simmons, J. Immunol. **115**, 1650 (1975).
[2] R. Gundersen and J. Barrett, Science **206**, 1079 (1979).
[3] S. Boyden, J. Exp. Med. **115**, 453 (1962).
[4] S. H. Zigmond, J. Cell Biol. **75**, 606 (1977).
[5] T. M. Keenan and A. Folch, Lab Chip **8**, 34 (2008).
[6] S. K. W. Dertinger, D. T. Chiu, N. L. Jeon, and G. M. Whitesides, Anal. Chem. **73**, 1240 (2001).
[7] D. Irimia, D. A. Geba, and M. Toner, Anal. Chem. **78**, 3472 (2006).
[8] N. L. Jeon, H. Baskaran, S. K. W. Dertinger, G. M. Whitesides, L. Van de Water, and M. Toner, Nat. Biotechnol. **20**, 826 (2002).
[9] B. G. Chung, L. A. Flanagan, S. W. Rhee, P. H. Schwartz, A. P. Lee, E. S. Monuki, and N. L. Jeon, Lab Chip **5**, 401 (2005).
[10] W. Saadi, S. J. Wang, F. Lin, and N. L. Jeon, Biomed. Microdevices **8**, 109 (2006).
[11] T. Ahmed, T. S. Shimizu, and R. Stocker, Integrative Biology **2**, 604 (2010).
[12] T. M. Keenan, C. Hsu, and A. Folch, Appl. Phys. Lett. **89**, 114103 (2006).
[13] A. Shamloo, N. Ma, M. Poo, L. L. Sohn, and S. C. Heilshorn, Lab Chip **8**, 1292 (2008).
[14] N. Bhattacharjee, N. Z. Li, T. M. Keenan, and A. Folch, Integrative Biology **2**, 669 (2010).
[15] V. V. Abhyankar, M. A. Lokuta, A. Huttenlocher, and D. J. Beebe, Lab Chip **6**, 389 (2006).
[16] T. Kim, M. Pinelis, and M. M. Maharbiz, Biomed. Microdevices **11**, 65 (2008).
[17] B. Mosadegh, M. Agarwal, H. Tavana, T. Bersano-Begey, Y. Torisawa, M. Morell, M. J. Wyatt, K. S. O'Shea, K. F. Barald, and S. Takayama, Lab Chip **10**, 2959 (2010).
[18] D. M. Cate, C. G. Sip, and A. Folch, Biomicrofluidics **4**, 044105 (2010).
[19] C. Hsu, C. Chen, and A. Folch, Lab Chip **4**, 420 (2004).
[20] D. Jowhar, G. Wright, P. C. Samson, J. P. Wikswo, and C. Janetopoulos, Integrative Biology **2**, 648 (2010).
[21] J. Diao, L. Young, S. Kim, E. A. Fogarty, S. M. Heilman, P. Zhou, M. L. Shuler, M. Wu, and M. P. DeLisa, Lab Chip **6**, 381 (2006).
[22] S. Cheng, S. Heilman, M. Wasserman, S. Archer, M. L. Shuler, and M. Wu, Lab Chip **7**, 763 (2007).
[23] H. Bang, W. G. Lee, J. Park, H. Yun, J. Lee, S. Chung, K. Cho, C. Chung, D. C. Han, and J. K. Chang, J. Micromech. Microeng. **16**, 708 (2006).
[24] B. G. Chung, J. W. Park, J. S. Hu, C. Huang, E. S. Monuki, and N. L. Jeon, BMC Biotechnology **7**, 60 (2007).
[25] U. Y. Schaff, M. M. Q. Xing, K. K. Lin, N. Pan, N. L. Jeon, and S. I. Simon, Lab Chip **7**, 448 (2007).
[26] I. Barkefors, S. Thorslund, F. Nikolajeff, and J. Kreuger, Lab Chip **9**, 529 (2009).
[27] Z. Zhang, P. Zhao, and G. Xiao, Polymer **50**, 5358 (2009).
[28] N. Y. Lee and B. H. Chung, Langmuir **25**, 3861 (2009).
[29] A. Bancaud, G. Wagner, K. D. Dorfman, and J. L. Viovy, Anal. Chem. **77**, 833 (2005).
[30] G. M. Walker, J. Sai, A. Richmond, M. Stremler, C. Y. Chung, and J. P. Wikswo, Lab Chip **5**, 611 (2005).